



## Two-phonon coupling to the antiferromagnetic phase transition in multiferroic BiFeO<sub>3</sub>

Mariola O. Ramirez, M. Krishnamurthi, S. Denev, A. Kumar, Seung-Yeul Yang, Ying-Hao Chu, Eduardo Saiz, Jan Seidel, A. P. Pyatakov, A. Bush, D. Viehland, J. Orenstein, R. Ramesh, and Venkatraman Gopalan

Citation: *Applied Physics Letters* **92**, 022511 (2008); doi: 10.1063/1.2829681

View online: <http://dx.doi.org/10.1063/1.2829681>

View Table of Contents: <http://scitation.aip.org/content/aip/journal/apl/92/2?ver=pdfcov>

Published by the AIP Publishing

---

### Articles you may be interested in

[Low temperature hydrothermal epitaxy and Raman study of heteroepitaxial BiFeO<sub>3</sub> film](#)  
Appl. Phys. Lett. **95**, 122509 (2009); 10.1063/1.3237160

[Magnetic, ferroelectric, and dielectric properties of Bi \(Sc<sub>0.5</sub>Fe<sub>0.5</sub>\)O<sub>3</sub> – PbTiO<sub>3</sub> thin films](#)  
J. Appl. Phys. **105**, 074101 (2009); 10.1063/1.3093691

[Effect of Ti substitution on multiferroic properties of BiMn<sub>2</sub>O<sub>5</sub>](#)  
J. Appl. Phys. **104**, 033707 (2008); 10.1063/1.2964072

[Substantial magnetoelectric coupling near room temperature in Bi<sub>2</sub>Fe<sub>4</sub>O<sub>9</sub>](#)  
Appl. Phys. Lett. **92**, 132910 (2008); 10.1063/1.2905815

[Multiferroicity in polarized single-phase Bi<sub>0.875</sub>Sm<sub>0.125</sub>FeO<sub>3</sub> ceramics](#)  
J. Appl. Phys. **100**, 024109 (2006); 10.1063/1.2220642

---



## Re-register for Table of Content Alerts

Create a profile.



Sign up today!



## Two-phonon coupling to the antiferromagnetic phase transition in multiferroic BiFeO<sub>3</sub>

Mariola O. Ramirez,<sup>1,a)</sup> M. Krishnamurthi,<sup>1</sup> S. Denev,<sup>1</sup> A. Kumar,<sup>1</sup> Seung-Yeul Yang,<sup>2</sup> Ying-Hao Chu,<sup>2</sup> Eduardo Saiz,<sup>3</sup> Jan Seidel,<sup>2</sup> A. P. Pyatakov,<sup>4</sup> A. Bush,<sup>5</sup> D. Viehland,<sup>6</sup> J. Orenstein,<sup>7</sup> R. Ramesh,<sup>2</sup> and Venkatraman Gopalan<sup>1,b)</sup>

<sup>1</sup>Department of Materials Science and Engineering and Materials Research Institute, Pennsylvania State University, University Park, Pennsylvania 16802, USA

<sup>2</sup>Department of Materials Science and Engineering and Department of Physics, University of California, Berkeley, California 94720-1760, USA

<sup>3</sup>Materials Sciences Division, Lawrence Berkeley National Laboratory, Berkeley, California 94720, USA

<sup>4</sup>Physics Department, Moscow State University, Leninskie gori, 38, Moscow 119992, Russia

<sup>5</sup>Moscow State Institute of Radio Engineering, Electronics and Automation, Vernadskii Prospect, 78, Moscow 117454, Russia

<sup>6</sup>Department of Materials Science and Engineering, Virginia Tech, Blacksburg, Virginia 24061, USA

<sup>7</sup>Department of Physics, University of California, Berkeley, California 94720-1760, USA

(Received 7 October 2007; accepted 6 December 2007; published online 16 January 2008)

A prominent band centered at  $\sim 1000$ – $1300$   $\text{cm}^{-1}$  and associated with resonant enhancement of two-phonon Raman scattering is reported in multiferroic BiFeO<sub>3</sub> thin films and single crystals. A strong anomaly in this band occurs at the antiferromagnetic Neel temperature,  $T_N \sim 375$  °C. This band is composed of three peaks, assigned to  $2A_4$ ,  $2E_8$ , and  $2E_9$  Raman modes. While all three peaks were found to be sensitive to the antiferromagnetic phase transition, the  $2E_8$  mode, in particular, nearly disappears at  $T_N$  on heating, indicating a strong spin-two-phonon coupling in BiFeO<sub>3</sub>.

© 2008 American Institute of Physics. [DOI: 10.1063/1.2829681]

Multiferroics, specially materials that combine spontaneous magnetic and ferroelectric order parameters, are currently the subject of intensive investigations because of their potential for electrical control of magnetism, and vice versa.<sup>1–5</sup> Bismuth ferrite, BiFeO<sub>3</sub> (BFO), is probably the most widely studied, since it exhibits multiferroicity at room temperature, with a coexistence of ferroelectricity and antiferromagnetism up to its Neel temperature of  $T_N \sim 375$  °C. At room temperature (RT), BFO is a rhombohedrally distorted ferroelectric perovskite with space group  $R3c$  and Curie temperature,  $T_C \sim 830$  °C.<sup>6</sup> It also shows a  $G$ -type canted antiferromagnetic (AFM) order below  $T_N$ .<sup>7</sup>

While ferroelectricity is relatively easier to study in this material, the probing of magnetism is more challenging.<sup>8</sup> In particular, the coupling between ferroelectricity and magnetism is of key significance. Several techniques, such as diffraction experiments,<sup>9</sup> second harmonic generation (SHG),<sup>10,11</sup> and recently Raman spectroscopy,<sup>12,13</sup> have been employed. Evidence of the strong magnetoelectric coupling has been demonstrated by the observation of electrical control of both ferroelectric and antiferromagnetic domains in BFO films at RT.<sup>14</sup> Last year, Haumont *et al.* reported pronounced phonon anomalies around  $T_N$  due to phonons influenced by spin correlations.<sup>12,13</sup> The reported Raman spectra by Haumont *et al.* have not fully agreed with other theoretical and experimental Raman studies on thin films, ceramics, or bulk BFO single crystals, suggesting variability between different samples.<sup>15–20</sup> The selection rules for the Raman active modes in rhombohedral  $R3c(C_{3v}^6)$  symmetry predict only 13 active Raman phonons with  $A_1$  and  $E$  symmetries, according to the irreducible representation,  $\Gamma_{\text{Raman/IR}} = 4A_1 + 9E$ . In

polarized Raman scattering, the  $A_1$  modes can be observed by parallel polarization, while the  $E$  modes can be observed by both parallel and crossed polarizations. Since all these modes fall in the frequency range below  $\sim 700$   $\text{cm}^{-1}$ , most of the Raman studies have focused in this region, with the subsequent lack of information at higher frequencies. In this letter, we present Raman spectra in the  $100$ – $2000$   $\text{cm}^{-1}$  spectral range in thin films and bulk single crystals. In addition to the well-understood Raman features in the low frequency region, the spectra show a very prominent band at  $\sim 1000$ – $1300$   $\text{cm}^{-1}$ , which we associate with two-phonon Raman scattering, strongly enhanced due to the resonance with the intrinsic absorption edge. The temperature dependence of the two-phonon contribution to the total Raman spectrum has been analyzed in the proximity of  $T_N$ . Remarkable changes in both intensity and spectral shape have been observed, pointing out the strong spin-two-phonon coupling in BFO.

$4.5$   $\mu\text{m}$  BiFeO<sub>3</sub> films on (110) DyScO<sub>3</sub> were grown by metal-organic chemical-vapor deposition equipped with a liquid delivery system.<sup>14</sup> The thick films were relaxed and have (001)<sub>*p*</sub> pseudocube-on-pseudocube epitaxial geometry with trigonal  $C_{3v}$  crystal structure. BiFeO<sub>3</sub> single crystals with (001)<sub>*p*</sub> crystal faces were grown in a sealed platinum crucible from a flux melt of Bi<sub>2</sub>O<sub>3</sub>, Fe<sub>2</sub>O<sub>3</sub>, and NaCl (75.6:17.9:6.5 molar ratio). Raman spectra were recorded in a backscattering geometry by using a WITec alpha 300 S confocal Raman microscope equipped with a Linkam heating stage. Low laser excitation power density ( $<1$  mW/area) was employed.

Figures 1(a) and 1(b) show the unpolarized Raman spectra as a function of temperature for the BiFeO<sub>3</sub> thin film and single crystal, respectively. As seen, both the thin films and the single crystal show the same Raman modes at similar

<sup>a)</sup>Electronic mail: mdr20@psu.edu.

<sup>b)</sup>Electronic mail: vgopalan@psu.edu.

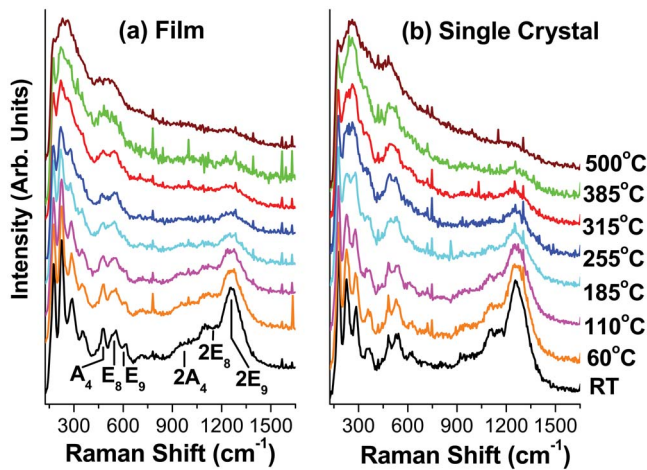


FIG. 1. (Color online) Temperature-dependent (room temperature to 550 °C) unpolarized Raman scattering spectra of BiFeO<sub>3</sub> film (a) and bulk single crystal (b) under excitation at 514 nm.

energy positions. When comparing the low frequency Raman modes in Fig. 1 (100–700 cm<sup>-1</sup>), with those previously theoretically and experimentally reported, good agreement is obtained. The only difference is the prominent additional band around ~1000–1300 cm<sup>-1</sup> which has not been reported before. Changing the excitation wavelength to 488 nm led to no observed spectral shifts in this band; therefore, its Raman scattering nature is confirmed. The origin of this structure has been assigned to the combination of three different two-phonon Raman overtones labeled 2A<sub>4</sub>, 2E<sub>8</sub>, and 2E<sub>9</sub>, since their spectral positions correspond to practically double the energy values of the A(LO<sub>4</sub>) ~480 cm<sup>-1</sup>, E(TO<sub>8</sub>) ~550 cm<sup>-1</sup>, and E(TO<sub>9</sub>) ~620 cm<sup>-1</sup> normal modes of BFO, respectively.<sup>15,16</sup> The strong contribution of the two-phonon band to the total Raman spectrum has been attributed to a resonant enhancement with the intrinsic absorption edge in BFO. This is similar to the two-phonon bands reported in hematite, α-Fe<sub>2</sub>O<sub>3</sub> the simplest case of iron oxides containing only FeO<sub>6</sub> octahedra.<sup>21–23</sup> As the samples are heated (Fig. 1), the Raman modes gradually broaden, as well as slightly shift to lower wavenumbers, which is expected due to thermal expansion and thermal disorder, respectively. The most striking feature, however, is a dramatic decrease in the total integrated intensity, as well as the spectral shape of the two-phonon Raman band with increasing temperature.

Figure 2 shows a detail of the Raman spectrum in the 700–1600 cm<sup>-1</sup> wavenumber region below (RT) and above (400 °C) the AFM phase transition in BFO. In both cases, the broad two-phonon overtone can be fitted into three Gaussian bands peaking at around 968, 1110, and 1265 cm<sup>-1</sup> at RT and 961, 1092, and 1258 cm<sup>-1</sup> at 400 °C, i.e., practically the double energy values of A<sub>4</sub>, E<sub>8</sub>, and E<sub>9</sub> normal modes in BFO. From the fit, the full width at half maximum of these bands was found to be 115, 123, and 145 cm<sup>-1</sup>, respectively, at RT and 145, 139, and 170 cm<sup>-1</sup> at 400 °C. The spectral shifts and broadening occur due to thermal dependence of Raman modes. At first sight, on comparing both spectra, a clear change in the spectral shape is observed, mainly due to the strong reduction of the 2E<sub>8</sub> contribution when passing through the AFM phase transition.

Figure 3 shows the total contribution to the Raman spectra of the most intense 2E<sub>9</sub> two-phonon band (center at ~1260 cm<sup>-1</sup>) as a function of temperature. In this figure, the

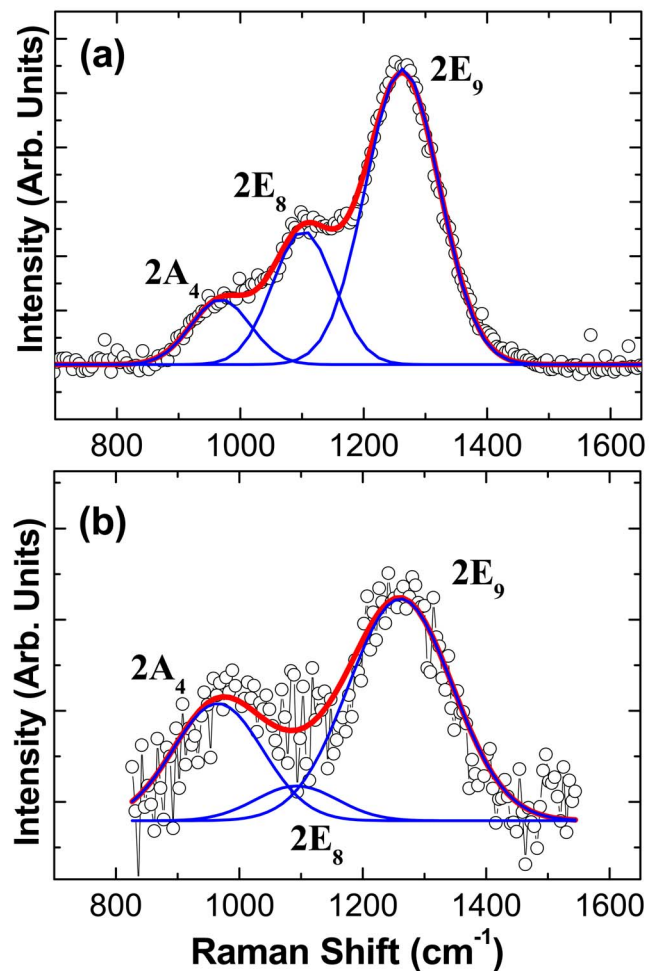


FIG. 2. (Color online) Detail of the Raman spectrum in the 700–1600 cm<sup>-1</sup> wavenumber region. Solid lines are fits to three Gaussian functions corresponding to two-phonon replica of the A<sub>4</sub>, E<sub>8</sub>, and E<sub>9</sub> normal modes in BFO, respectively. (a) Room temperature and (b) T=400 °C.

intensity of the two-phonon scattering  $I_{2P}$  has been normalized to the one-phonon scattering intensity  $I_P$  of the Raman active mode at 254 cm<sup>-1</sup> and reduced by the appropriate thermal population factor,

$$R = I_{2P}[n(\omega_p) + 1]/I_P[n(\omega_{2p}) + 1]^2, \quad (1)$$

where  $n(\omega) = (e^{h\omega/kT} - 1)^{-1}$  is the Bose-Einstein factor. By using the reduced Raman intensity given by  $R$ , the contribution of the Bose-Einstein population from the measured Raman intensity is eliminated, and the intensity changes can be compared independent of the population considerations. On approaching  $T_N$ , a remarkable decrease in the temperature dependence of the integrated intensity of the two-phonon Raman scattering in BiFeO<sub>3</sub> is seen, followed by a constant value after the AFM phase transition. Similar results were obtained when the integrated intensity corresponding to the other two-phonon overtone center at 965 and 1110 cm<sup>-1</sup> was analyzed. Therefore, a strong interplay between the ferroelectric and magnetic subsystems of BFO can be concluded. We particularly note the high sensitivity of the two-phonon band to the AFM phase transition in BFO as compared to the one-phonon scattering mode, since its total contribution to the Raman spectrum was referred (normalized) to the one-phonon band. Figure 3 also shows the ratio between 2E<sub>8</sub> and 2E<sub>9</sub> two-phonon scattering integrated intensity

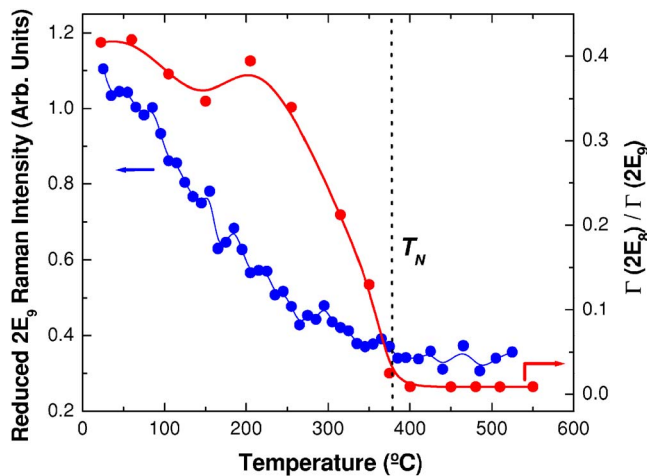


FIG. 3. (Color online) (Left axis) Temperature dependence of the reduced integrated Raman intensity of the  $1260\text{ cm}^{-1}$  two-phonon Raman scattering band in  $\text{BiFeO}_3$  normalized to scattering intensity of the  $254\text{ cm}^{-1}$  phonon. (Right axis) Integrated intensity ratio between  $2E_8$  and  $2E_9$  two-phonon modes, as a function of the sample temperature.

$\Gamma(2E_8)/\Gamma(2E_9)$ , as a function of temperature. As can be seen, it remains almost constant up to  $\sim 200^\circ\text{C}$  and abruptly decreases in the vicinity of  $T_N$ , supporting again the significant spin-two-phonon coupling in BFO.

A plausible model to explain this behaviour may relate to the specific bond motion of the Raman modes and the octahedral rotation along the  $[111]$  axis responsible of the weak ferromagnetism in BFO.<sup>24</sup> Previous studies on the assignment of the Raman modes in BFO thin films with pseudotetragonal symmetry attributes the  $A_1$  modes and the low frequency  $E$  modes ( $<400\text{ cm}^{-1}$ ) to Bi–O1 bonds. The higher frequency  $E$  modes are attributed to Fe–O bonds. Most specifically, some of them are related to Fe–O1 and others with Fe–O2, where O1 are axial and O2 are equatorial ions.<sup>17</sup> This assignment also agrees with other Raman scattering studies on  $\text{Bi}_{1-x}\text{Nd}_x\text{FeO}_3$  multiferroic ceramics where a change of Bi–O covalent bonds is observed with increasing  $x$ .<sup>15</sup> Therefore, from the results displayed in Fig. 2, we can tentatively assign the  $2E_8$  overtone to Fe–O1 bonding and the  $2E_9$  to Fe–O2 and hence relate it with the octahedral rotation critical to weak magnetism. Oxygen rotation plays an important role in the antiferromagnetism through superexchange, which is very dependent on bond angles. Thus, if there is spin-phonon coupling, the structural distortions due to the AFM order should be reflected in the evolution of Raman scattering spectra, which might explain the different evolutions of the two-phonon overtones on approaching  $T_N$  (see Fig. 3). We also note a recent work that reassigns the Raman mode at  $550\text{ cm}^{-1}$  as  $A_1(\text{TO})$  transversal mode since it was only observed in parallel polarized pump and Raman signals geometry.<sup>25</sup> Though we cannot ascertain the new assignment in this study, the plausible explanation proposed could also account for this new assignment since a slight spin-phonon coupling to the AFM phase transition is predicted for both the  $A_1(\text{TO})$  and  $E(\text{TO})$  modes by first principle calculations.<sup>18,26</sup>

In summary, a resonant enhancement of two-phonon Raman scattering in the vicinity of  $1200\text{ cm}^{-1}$  has been re-

ported in BFO multiferroic system. Temperature studies well above the Neel temperature show a strong coupling of the two-phonon band to the AFM phase transition in BFO. Significant changes in the integrated intensity as well as in the spectral shape when approaching  $T_N$  were observed. Additionally, since no dramatic changes—excepting for the intensity variations above mentioned—were observed in the overall Raman spectrum when crossing  $T_N$ , it is possible to conclude that the antiferromagnetic phase transition in BFO does not seem to be accompanied by dramatic structural changes. From the results presented in this work, it is clear that spin-phonon coupling, as well as the temperature dependence of the ferroelectric order parameter cannot be neglected in the proximity of  $T_N$ .

We acknowledge funding from the National Science Foundation under Grant Nos. DMR-0512165, DMR-0507146, DMR-0213623, and DMR-0602986.

- <sup>1</sup>T. Kimura, T. Goto, H. Shintani, K. Ishizaka, T. Arima, and Y. Tokura, *Nature (London)* **426**, 55 (2003).
- <sup>2</sup>N. Hur, S. Park, P. A. Sharma, J. S. Ahn, S. Guha, and S. W. Cheong, *Nature (London)* **429**, 392 (2004).
- <sup>3</sup>N. A. Spaldin and M. Fiebig, *Science* **309**, 391 (2005).
- <sup>4</sup>W. Erenstein, N. D. Mathur, and J. F. Scott, *Nature (London)* **442**, 759 (2006).
- <sup>5</sup>M. Fiebig, Th. Lottermoser, D. Frohlich, A. V. Goltsev, and R. V. Pisarev, *Nature (London)* **419**, 818 (2002).
- <sup>6</sup>F. Kubel and H. Schmid, *Acta Crystallogr., Sect. B: Struct. Sci.* **46**, 698 (1990).
- <sup>7</sup>P. Fischer, M. Polomska, I. Sosnowska, and M. Szymanski, *J. Phys. C* **13**, 1931 (1980).
- <sup>8</sup>M. Fiebig, V. V. Palov, and R. V. Pisarev, *J. Opt. Soc. Am. B* **22**, 96 (2005).
- <sup>9</sup>A. Pawelicz, R. Przenioslo, I. Sosnowska, and A. W. Hewat, *Acta Crystallogr., Sect. B: Struct. Sci.* **63**, 537 (2007).
- <sup>10</sup>A. M. Agaltsov, V. S. Gorelik, A. K. Zvezdin, V. A. Murashov, and D. N. Rakov, *Sov. Phys. Short Commun.* **5**, 37 (1989).
- <sup>11</sup>M. S. Kartavtseva, O. Yu. Gorbenko, A. R. Kaul, T. V. Murzina, S. A. Savinov, and O. A. Aktsipetrov, *J. Mater. Res.* **22**, 2063 (2007).
- <sup>12</sup>R. Haumont, J. Kreisel, P. Bouvier, and F. Hippert, *Phys. Rev. B* **73**, 132101 (2006).
- <sup>13</sup>R. Haumont, J. Kreisel, and P. Bouvier, *Phase Transitions* **79**, 1043 (2006).
- <sup>14</sup>T. Zhao, A. Scholl, F. Zavaliche, K. Lee, M. Barry, A. Doran, M. P. Cruz, Y. H. Chu, C. Ederer, N. A. Spaldin, R. R. Das, D. M. Kim, S. H. Baek, C. B. Eom, and R. Ramesh, *Nat. Mater.* **5**, 823 (2006).
- <sup>15</sup>G. L. Yuan, S. W. Or, and H. L. Wa Chan, *J. Appl. Phys.* **101**, 064101 (2007).
- <sup>16</sup>M. K. Singh, H. M. Jang, S. Ryu, and M. Jo, *Appl. Phys. Lett.* **88**, 042907 (2006).
- <sup>17</sup>M. K. Singh, S. Ryu, and H. M. Jang, *Phys. Rev. B* **72**, 132101 (2005).
- <sup>18</sup>P. Hermet, M. Goffinet, J. Kreisel, and Ph. Ghosez, *Phys. Rev. B* **75**, 220102 (2007).
- <sup>19</sup>H. Fukumura, H. Harima, K. Kisoda, M. Tamada, Y. Noguchi, and M. Miyayama, *J. Magn. Magn. Mater.* **310**, e367 (2007).
- <sup>20</sup>S. Kamba, D. Nuzhnyy, M. Savinov, J. Sebek, J. Petzelt, J. Prokleska, R. Haumont, and J. Kreisel, *Phys. Rev. B* **75**, 024403 (2007).
- <sup>21</sup>K. F. McCarty, *Solid State Commun.* **68**, 799 (1988).
- <sup>22</sup>T. P. Martin, R. Merlin, D. R. Huffman, and M. Cardona, *Solid State Commun.* **22**, 565 (1977).
- <sup>23</sup>M. J. Massey, U. Baier, R. Merlin, and W. H. Weber, *Phys. Rev. B* **41**, 7822 (1990).
- <sup>24</sup>C. Ederer and N. A. Spaldin, *Phys. Rev. B* **71**, 060401 (2005).
- <sup>25</sup>M. Cazayous, D. Malka, D. Lebeugle, and D. Colson, *Appl. Phys. Lett.* **91**, 071910 (2007).
- <sup>26</sup>C. Fennie and C. Ederer (private communication).